Prepared for submission to JHEP LAPTH-012/16, IPPP/16/22, DCPT/16/44

The Lepton Flavour Violating Higgs Decays at the HL-LHC and the ILC

Shankha Banerjee[1], **Biplob Bhattacherjee**[2], **Manimala Mitra**[3], **Michael Spannowsky**[4]

[1] *LAPTH, Univ. de Savoie, CNRS, B.P.110, F-74941 Annecy-le-Vieux, France*

[2] *Centre for High Energy Physics, Indian Institute of Science, 560012 Bangalore, INDIA*

[3] *Indian Institute of Science Education and Research Mohali, Knowledge city, Sector 81, SAS Nagar, Manauli PO 140306.*

[4] *Institute for Particle Physics Phenomenology, Durham University, Durham DH1 3LE, United Kingdom.*

Abstract: Run-I results from the CMS collaboration show an excess of events in the decay $h \to \mu\tau_e$ with a local significances of 2.4σ. This could be the first hint of flavour violation in the Higgs sector. We summarise the bounds on the flavour violating Yukawa couplings from direct searches, low energy measurements and projected future experiments. We discuss the sensitivity of upcoming HL-LHC runs and future lepton colliders in measuring lepton-flavour violating couplings using an effective field theory framework. For the HL-LHC we find limits on $\mathrm{BR}(h \to \mu\tau)$ and $\mathrm{BR}(h \to e\tau) \lesssim \mathcal{O}(0.5)\%$ and on $\mathrm{BR}(h \to e\mu) \lesssim \mathcal{O}(0.02)\%$. For an ILC with center-of-mass energy of 1 TeV we expect $\mathrm{BR}(h \to e\tau)$ and $\mathrm{BR}(h \to \mu\tau)$ to be measurable down to $\mathcal{O}(0.2)\%$.

arXiv:1603.05952v2 [hep-ph] 29 Jun 2016

Contents

1 Introduction **1**

2 Higgs couplings in the lepton sector **3**
2.1 Present status of Higgs couplings in the lepton sector 4
2.1.1 Limits from direct searches 4
2.1.2 Limits from low-energy measurements 5
2.1.3 Future limits 6

3 Direct detection of LFV at the HL-LHC **9**
3.1 Prospect of $\mu\tau$ channel 10
3.2 Prospect of $e\tau$ channel 11
3.3 Prospect of $e\mu$ 15

4 $h \to e\tau$ at ILC **15**
4.1 ILC at $\sqrt{s} = 250$ GeV 17
4.2 ILC at $\sqrt{s} = 1$ TeV 17

5 Summary **20**

1 Introduction

The Large Hadron Collider (LHC) has successfully discovered a scalar resonance of mass around 125 GeV [1, 2], with properties in close agreement with the Standard Model (SM) Higgs boson. Already now, both ATLAS and CMS collaborations have established its couplings to massive gauge bosons and photons to a high degree of precision and found no significant deviations from SM predictions [3–5].

Direct limits on rather complex Higgs-fermion interactions were instead much less probed during initial LHC runs. Only fairly weak limits were obtained on Higgs couplings to b-quarks [3], τ-leptons [6, 7] and t-quarks [8–12]. Albeit the good overall agreement between theory and experiment, i.e. the total signal strength measured from production and decay modes is $\mu = 1.09 \pm 0.11$ [3], more conclusive evidence is required to establish that the observed scalar resonance is indeed the SM Higgs boson.

In particular the Higgs decays to the first and second generation fermions are yet to be observed. While searches have been performed by ATLAS and CMS to measure the Higgs decays to a $\mu^+\mu^-$ pair [13, 14] and by CMS to an e^+e^- pair [14], only upper limits have been obtained so far. Indirect limits on these decays could be potentially obtained from a very precise measurement of the total Higgs decay width. While future linear colliders can play an important role in this [15, 16], at present, the Higgs width is only fairly loosely

bounded to $\Gamma_H < 22$ MeV (22.7 MeV) at 95% C.L from CMS (ATLAS) [17, 18] using highly model-dependent off-shell coupling measurements [19, 20]. Further, a global coupling fit to Higgs data indicates that the Higgs boson can have a sizable non-standard branching fraction, *i*.e. $\mathrm{BR}_{\text{non-std}} < 0.26$ at 95% C.L [21]. Hence, within the present experimental findings exotic Higgs decays into first and second-generation fermions, gluons or missing energy can be significantly enhanced compared to SM predictions.

Among the many different plausible non-standard decay modes of the Higgs boson, one of the most intriguing are flavour violating Higgs decays. In the SM, these decays are highly suppressed, thus any experimental confirmation of such a process will be conclusive evidence of physics beyond the standard model (BSM). During run-I of the LHC, a number of searches have been carried out both by CMS [22, 23] and ATLAS [24, 25]. The result reported by CMS constrains the branching ratio $\mathrm{BR}(h \to \mu\tau) < 1.51$ % at 95% C.L, while the upper limit on the branching ratio reported by ATLAS is 1.43%. Remarkably, both CMS and ATLAS reported a mild excess in the $h \to \mu\tau_e$ channel with a local significances of 2.4σ and 1.3σ respective[1]. These results can be explained with the best-fit branching ratio of $\mathrm{BR}(h \to \tau\mu) = 0.84\%(0.77\%)$ for CMS (ATLAS). In addition, CMS also looked for flavour violation in the $e\mu$ and $e\tau$ channels [23]. Recently, ATLAS updated their results from the $h \to e\tau$ analysis at 8 TeV [24].

Apart from direct searches, flavour violating interactions of the Higgs boson can also be measured in low-energy observables, e.g. $\mu \to e\gamma$, $\tau \to \mu\gamma$, $\tau \to e\gamma$, $\tau \to 3e$, $\mu \to 3e$ and $\mu - e$ conversion in nuclei. For a detailed discussion, see Refs. [26, 27]. Hence, non-observation of these processes puts additional constraints on flavour violating couplings [26–28].

Assuming the low energy dynamics can be described in terms of an effective field theory (EFT), flavour violation in the Higgs sector is highly correlated with flavour violation in low energy processes [26–29]. However, in the presence of light degrees of freedom, this correlation might not hold. There have been several attempts to construct concrete models that can explain large branching ratios of the Higgs into non-degenerate fermion flavours, while simultaneously satisfying all low energy constraints. Lepton flavour violating Higgs decays have been discussed in the context of supersymmetry [30–34], extended Higgs sectors [35–50] and other BSM models [51–64]. Some collider aspects in the flavour violating sector have been studied in Refs. [65–69].

Thus, motivated by the recent searches carried out by CMS and ATLAS, we present a detailed analysis of flavour violation in direct and indirect experimental searches and compare their sensitivities. We first review the different experimental constraints on Higgs lepton-flavour violating and non-violating couplings in section 2. Here we also discuss some of the future limits of low energy experiments, e.g. MEG-II, Belle-II and super KEKB. After establishing the reach of low energy constraints using an EFT framework, we study the sensitivity of future high luminosity LHC runs on lepton flavour violating decays in section 3. We provide a case study for $h \to e\tau$ at the ILC in section 4. In sections 3

[1] ATLAS has studied 2 signal regions and the local significance in one of the signal regions (SR2) is about 2.2σ.

and 4, we consider the respective LFV branching ratios as free parameters and evaluate how well they can be constrained in collider measurements. Finally we discuss our findings and summarise them in section 5.

2 Higgs couplings in the lepton sector

In the SM, the Yukawa couplings are proportional to the masses of the fermions. Confirmation of this hypothesis requires independent measurements of the fermion masses and their coupling strength to the Higgs boson. That is a strenuous task, particularly for the Higgs boson couplings to the first and second generation fermions. A precise statement about the relation between Yukawa couplings and fermion masses is still at stake. Because of the observation of the recent excess reported by CMS in the $h \to \mu\tau$ channel, we are restricting ourselves to a study of LFV interactions[2]. In this section we review and update the existing searches on such LFV decays and summarise their bounds.

To give an interpretation of the measurements in terms of LFV interactions we consider an effective theory where the interaction between Higgs and fermions are given by the Yukawa interactions

$$\mathcal{L}_Y = -m_i \bar{f_L^i} f_R^i - Y_{ij}(\bar{f_L^i} f_R^j)h + \ h.c.. \tag{2.1}$$

where we use $Y_{ii} = \frac{m_i}{v}$ and f_L and f_R are the charged leptons. The Yukawa coupling matrix is parametrised [27] by

$$Y_{ij} = \frac{m_i}{v}\delta_{ij} + \frac{v^2}{\sqrt{2}\Lambda^2}\hat{\lambda}_{ij}, \tag{2.2}$$

with $\hat{\lambda} = V_L \lambda^{'} V_R$. V_L and V_R are unitary matrices which diagonalise the mass matrix after electroweak symmetry breaking (EWSB) and $-\frac{\lambda^{'}_{ij}}{\Lambda^2}$ are the coefficients of the gauge invariant dimension-6 operators,

$$\Delta\mathcal{L}_Y = -\frac{\lambda^{'}_{ij}}{\Lambda^2}\bar{F_L^i} F_R^j H(H^\dagger H) + \ h.c, \tag{2.3}$$

where F_L is the fermion doublet, F_R is the singlet and H is the SM scalar doublet. For $\Lambda \to \infty$, we recover the SM Yukawa structure. There are also some gauge invariant dimension-6 operators involving derivatives, induced by [27]

$$\Delta\mathcal{L}_D = \frac{\lambda_L^{ij}}{\Lambda^2}(\bar{F_L^i}\gamma^\mu F_L^j)(H^\dagger i\overleftrightarrow{D_\mu} H) + \frac{\lambda_R^{ij}}{\Lambda^2}(\bar{F_R^i}\gamma^\mu F_R^j)(H^\dagger i\overleftrightarrow{D_\mu} H), \tag{2.4}$$

with $H^\dagger i\overleftrightarrow{D_\mu} H = H^\dagger i D_\mu H - (iD_\mu H^\dagger)H$. However, these operators do not contribute to the $Hf\bar{f}$ couplings as shown in Eq. 2.1 after EWSB and hence we disregard further discussions of these operators in the present study[3].

[2] A detailed study on the flavour violating Higgs in the quark sector has been discussed, for example in Ref. [27].

[3] In Ref. [28], LFV has also been studied in the context of dipole operators of the form $H\bar{f}\sigma^{\mu\nu}fV_{\mu\nu}$. Such operators can induce flavour violating three body decays of the Higgs boson. However, precision constraints are stringent and render the prospects of discovering these decays at collider experiments slim.

2.1 Present status of Higgs couplings in the lepton sector

We list the current constraints on the Higgs Yukawa couplings in the lepton sector. First, we briefly summarise the status of the flavour diagonal and off-diagonal leptonic decays from direct searches during run-I at the LHC. Next we discuss the low energy constraints on the LFV Yukawas in an EFT framework.

2.1.1 Limits from direct searches

- $h \to e^+e^-$: An upper limit on its branching ratio has been obtained by CMS [14] of $\text{BR}(h \to e^+e^-) < 0.19\%$, which is about 3.7×10^5 times that of the SM expectation.

- $h \to \mu^+\mu^-$: ATLAS and CMS obtain an upper limit on the branching ratio of $\text{BR}(h \to \mu^+\mu^-) < 0.15\%$ [13] and $\text{BR}(h \to \mu^+\mu^-) < 0.16\%$ [14] respectively.

- $h \to \tau^+\tau^-$: Both ATLAS [6] and CMS [7] have measured the Higgs boson coupling to a pair of τ leptons. For $m_h = 125.36\,\text{GeV}$ (125 GeV), ATLAS (CMS) has measured a signal strength of $1.43^{+0.43}_{-0.37}$ (0.78 ± 0.27) in this channel.

- $h \to e\mu$: CMS [23] sets a limit on $\text{BR}(h \to e\mu) < 0.036\%$ at 95% CL. One thus obtains

$$\sqrt{|Y_{e\mu}|^2 + |Y_{\mu e}|^2} < 5.43 \times 10^{-4}. \tag{2.5}$$

- $h \to e\tau$: CMS [23] studied the $h \to e\tau_\mu$ and $h \to e\tau_{had}$ channels and obtained better sensitivity than the current indirect limits. They find $\text{BR}(h \to e\tau) < 0.69\%$ at 95% CL. From this limit one deduces

$$\sqrt{|Y_{e\tau}|^2 + |Y_{\tau e}|^2} < 2.41 \times 10^{-3}. \tag{2.6}$$

  On the other hand, ATLAS obtained a weaker limit $\text{BR}(h \to e\tau) < 1.04\%$ at 95% CL [24].

- $h \to \mu\tau$: The search was conducted in the channel $pp \to h \to \mu\tau$, followed by the leptonic as well as hadronic decays of τ. CMS reported a slight excess of events around $m_h = 125$ GeV in the $h \to \mu\tau_e$ channel with a local significance of 2.4σ [22]. From this they obtained $\text{BR}(h \to \mu\tau) < 1.51\%$ at 95% CL with a best-fit of $(0.84^{+0.39}_{-0.37})\%$. ATLAS has set an upper limit of 1.43% on this branching ratio at 95% CL [24]. From the upper limit on $\text{BR}(h \to \mu\tau)$ from CMS one obtains

$$\sqrt{|Y_{\mu\tau}|^2 + |Y_{\tau\mu}|^2} < 3.6 \times 10^{-3}. \tag{2.7}$$

  In our calculation, we have used that the partial decay width of 125 GeV Higgs into two fermions is,

$$\Gamma(h \to \ell_\alpha \ell_\beta) = \frac{m_h}{8\pi}(|Y_{\ell_\alpha \ell_\beta}|^2 + |Y_{\ell_\beta \ell_\alpha}|^2), \tag{2.8}$$

where $\ell_\alpha = \ell_\beta = e, \mu, \tau$ and $\alpha \neq \beta$. The branching ratio for this decay mode is

$$\mathrm{BR}(\mathrm{h} \to \ell_\alpha \ell_\beta) = \frac{\Gamma(\mathrm{h} \to \ell_\alpha \ell_\beta)}{\Gamma_{\mathrm{SM}} + \Gamma(\mathrm{h} \to \ell_\alpha \ell_\beta)}, \tag{2.9}$$

where $\Gamma_{\mathrm{SM}} = 4.1$ MeV.

2.1.2 Limits from low-energy measurements

We motivate below the different bounds on these Yukawa couplings that emerge from the low energy flavour violating processes and summarise these limits in Table 1.

- $Y_{\mu\tau}$ is constrained by the non-observation of processes like $\tau \to \mu\gamma$ and $\tau \to 3\mu$. The branching ratio of the process $\tau \to \mu\gamma$ is bounded by $\mathrm{BR}(\tau \to \mu\gamma) < 4.4 \times 10^{-8}$ at 90% C.L. [70, 71]. Assuming the low energy dynamics to be governed by the two flavour violating couplings $Y_{\mu\tau}$ and $Y_{\tau\mu}$, the decay width of this process reads as [27]

$$\Gamma(\tau \to \mu\gamma) = \frac{\alpha m_\tau^5}{64\pi^4}(|c_L|^2 + |c_R|^2), \tag{2.10}$$

  where the Wilson coefficients, c_L and c_R at one loop are given by

$$c_{L(R)} \sim \frac{1}{3m_h^2} Y_{\tau\tau} Y_{\tau\mu} \left(-1 + \frac{3}{4}\log\frac{\mathrm{m_h^2}}{\mathrm{m_\tau^2}}\right). \tag{2.11}$$

  In the above expression, for simplicity, we assume that $Y_{\tau\mu} = Y_{\mu\tau}$. Higher-order corrections to $c_{L/R}$ receive contributions from the top Yukawa coupling and hence can be large [27]. For example, including two-loop contributions, $c_{L/R}$ increases by a factor $\mathcal{O}(4)$. For a full discussion on the dependence of Y_{tt} we refer to Ref. [27]. Hence by assuming $Y_{\tau\mu} = Y_{\mu\tau}$ and also a SM-like $Y_{\tau\tau}$, we obtain $Y_{\mu\tau} \lesssim 0.011$.

  In presence of flavour violating Yukawa interactions, the process $\tau \to 3\mu$ has a decay width of

$$\Gamma(\tau \to 3\mu) = \frac{\alpha^2 m_\tau^5}{6(2\pi)^5}(|c_L|^2 + |c_R|^2). \tag{2.12}$$

  Taking into account the one-loop contribution, the constraint on the Yukawa coupling is, $Y_{\mu\tau} < 0.177$. Similar to the previous limit, this also depends on the couplings $Y_{\tau\tau}, Y_{\mu\mu}$ and Y_{tt} and their SM values have been assumed in deriving the limit on $Y_{\mu\tau}$. This limit is weaker than $\tau \to \mu\gamma$ due to an additional factor of α (where α is the fine-structure constant).

- The coupling $Y_{\tau e}$ is also constrained from similar low energy flavour violating processes, such as, $\tau \to e\gamma$ and $\tau \to 3e$. The decay width for $\tau \to e\gamma$ has a similar expression as given in Eq. 2.10, where μ has to be replaced by e [27]. Under similar assumptions, one obtains $Y_{\tau e} \lesssim 0.01$ from $\tau \to e\gamma$, while from $\tau \to 3e$, this is relaxed owing to the extra α factor. Assuming $Y_{\tau e} = Y_{e\tau}$, we show the bounds on the Yukawas in Table. 1.

- The Yukawa coupling $Y_{\mu e}$ is severely constrained by the $\mu \to e\gamma$ limit from MEG [72]. The Wilson coefficients have similar expression as given in Eq. 2.10, with $\{\tau, \mu\} \to \{\mu, e\}$. The two loop contribution proportional to the top Yukawa coupling can be large [27]. The updated limit on the branching ratio, *viz.*, $\text{BR}(\mu \to e\gamma) < 5.7 \times 10^{-13}$ [70] imposes a tight constraint on the Yukawa $\sqrt{|Y_{\mu e}|^2 + |Y_{e\mu}|^2} \lesssim 1.75 \times 10^{-6}$. Assuming, $Y_{\mu e} = Y_{e\mu}$ this constrains $Y_{\mu e} \lesssim 1.24 \times 10^{-6}$. The other LFV process,*i.e*, $\mu \to 3e$ constrains $Y_{\mu e} \lesssim 2.19 \times 10^{-5}$.

- In addition to the above constraints, for complex Yukawa couplings, severe constraints appear from the electric dipole moment measurement. The electric dipole moment for the electron is $|d_e| \leq 10.5 \pm 0.07 \times 10^{-26} e$ cm [70], which constrains the complex Yukawas $|\text{Im}(Y_{e\tau} Y_{\tau e})| \lesssim 1.1 \times 10^{-8}$ and, $|\text{Im}(Y_{e\mu} Y_{\mu e})| \lesssim 9.8 \times 10^{-8}$.

  From the electric dipole measurement of muons, we have $-10 \times 10^{-20} e$ cm $< d_\mu < 8 \times 10^{-20} e$ cm [73]. This puts a weak constraint on $-0.8 \lesssim |\text{Im}(Y_{\mu\tau} Y_{\tau\mu})| \lesssim 1.0$ [27].

- The stringent constraint on $\mu \to e\gamma$ branching ratio can also be used to set the limit on the product of the flavour violating couplings $Y_{\tau\mu}$ and $Y_{\tau e}$. The limit from MEG, $\text{BR}(\mu \to e\gamma) < 5.7 \times 10^{-13}$ [70], imposes the constraint $(|Y_{\tau\mu} Y_{e\tau}|^2 + |Y_{\mu\tau} Y_{\tau e}|^2)^{\frac{1}{4}} < 2.373 \times 10^{-4}$ at one loop level. Again assuming $Y_{\tau\mu} = Y_{\mu\tau}$ and $Y_{\tau e} = Y_{e\tau}$, one obtains, $Y_{\tau\mu} Y_{e\tau} \lesssim 3.98 \times 10^{-8}$. Note that, in the limit $Y_{\mu e} = 0$, the two loop Barr-Zee diagram does not occur in this case.

- Besides, there are also constraints on the LFV Yukawa couplings from muonium-antimuonium oscillations [74, 75], magnetic dipole moments [76, 77] and from $\mu \to e$ conversions in nuclei [27, 78]. Furthermore, there are constraints from LEP which excludes $\sqrt{|Y_{\ell e}|^2 + |Y_{e\ell}|^2} <$ few $\times 10^{-1}$ [79]. These constraints are tabulated in Table 1. For a detailed review on these constraints, we refer the reader to Ref. [27].

2.1.3 Future limits

In this subsection we briefly discuss the expected future limits on the flavour diagonal and flavour violating couplings of the Higgs boson in the lepton sector.

- $h \to e^+ e^-$: Ref. [80] discusses the present and future bounds on the Y_{ee} Yukawa coupling. The ACME bound on the EDM puts a strong constraint on the imaginary part of this Yukawa, i.e. $< 1.7 \times 10^{-2}$ times the SM electron Yukawa, Y_e. The deviations of the real part are far less constrained. The authors find that the constraint coming from 8 TeV LHC data is the strongest. A limit $\kappa_e < 611$ can be derived, where κ_e is a multiplicative complex parameter to the SM Yukawa, which parametrises the deviation from the SM Yukawa coupling. Noting that for the 14 TeV run, the production cross-section of the Higgs will increase by a factor of ~ 2.5, they project that $\kappa_e \sim 260(150)$ with $\mathcal{L} = 300(3000)\,\text{fb}^{-1}$. For a 100 TeV pp collider with $\mathcal{L} = 3000\,\text{fb}^{-1}$, $\kappa_e \sim 75$.

Searches	Experimental limit on branching ratios	Limits on Yukawas
$\tau \to \mu\gamma$	4.4×10^{-8} [70, 71]	$Y_{\mu\tau} < 0.011$
$\tau \to 3\mu$	2.1×10^{-8} [70, 71]	$Y_{\mu\tau} < 0.176$
Muon EDM	$-10 \times 10^{-20} e$ cm $< \lvert d_\mu \rvert < 8 \times 10^{-20} e$ cm [73]	$-0.8 \lesssim \lvert \mathrm{Im}(\mathrm{Y}_{\mu\tau}\mathrm{Y}_{\tau\mu}) \rvert \lesssim 1.0$
Muon $g-2$	–	$\mathrm{Re}(\mathrm{Y}_{\mu\tau}\mathrm{Y}_{\tau\mu}) < (2.7 \pm 0.75) \times 10^{-3}$
$\tau \to \mu\gamma$ (f) (Belle-II/super KEKB)	10^{-9} [85]	$Y_{\mu\tau}$ <0.0017
$\tau \to e\gamma$	3.3×10^{-8} [70, 71]	$Y_{e\tau}$ <0.0099
$\tau \to 3e$	2.7×10^{-8} [70, 71]	$Y_{e\tau} < 0.085$
Electron $g-2$	–	$\mathrm{Re}(\mathrm{Y}_{e\tau}\mathrm{Y}_{\tau e}) < [-2.1, 2.9] \times 10^{-3}$
Electron EDM	$\lvert d_e \rvert \leq 0.105 \times 10^{-26}$ e cm	$\lvert \mathrm{Im}(\mathrm{Y}_{e\tau}\mathrm{Y}_{\tau e}) \rvert < 1.1 \times 10^{-8}$
$\tau \to e\gamma$ (f) (Belle-II/super KEKB)	10^{-9} [85]	$Y_{e\tau}$ <0.00172
$\mu \to e\gamma$	5.7×10^{-13} [70, 71]	$Y_{\mu e} < 1.24 \times 10^{-6}$
$\mu \to 3e$	1.0×10^{-12} [70, 71]	$Y_{\mu e} < 2.19 \times 10^{-5}$
Electron $g-2$	–	$\mathrm{Re}(\mathrm{Y}_{e\mu}\mathrm{Y}_{\mu e}) < [-0.019, 0.026]$
Electron EDM	$\lvert d_e \rvert \leq 0.105 \times 10^{-26}$ e cm	$\lvert \mathrm{Im}(\mathrm{Y}_{e\mu}\mathrm{Y}_{\mu e}) \rvert < 9.8 \times 10^{-8}$
$\mu \to e$ conversion	–	$Y_{\mu e} < 8.49 \times 10^{-6}$
$M - \bar{M}$ oscillations	–	$\lvert Y_{\mu e} + Y^*_{e\mu} \rvert < 0.079$
$\mu \to e\gamma$ (f) (MEG-II)	4×10^{-14} [84]	$Y_{\mu e}$ <3.28 $\times 10^{-7}$
$\mu \to e\gamma$	5.7×10^{-13}	$Y_{\mu\tau}Y_{e\tau}$ <3.98 $\times 10^{-8}$
$h \to \tau\mu$ (CMS)	1.51% [22]	$Y_{\mu\tau} < 2.55 \times 10^{-3}$
	0.84%	$Y_{\mu\tau} = 1.87 \times 10^{-3}$
$h \to \tau\mu$ (ATLAS)	1.43% [24]	$Y_{\mu\tau} < 2.45 \times 10^{-3}$
	0.77% [25]	$Y_{\mu\tau} = 1.79 \times 10^{-3}$
$h \to \tau\mu$ (CMS)+ $\mu \to e\gamma$	0.84%, 5.7×10^{-13}	$Y_{e\tau} < 2.13 \times 10^{-5}$
$h \to \tau\mu$ (ATLAS)+ $\mu \to e\gamma$	0.77%, 5.7×10^{-13}	$Y_{e\tau} < 2.23 \times 10^{-5}$
$h \to \tau e$ (CMS)	0.69% [23]	$Y_{e\tau} < 1.69 \times 10^{-3}$
$h \to \tau e$ (ATLAS)	1.04% [24]	$Y_{e\tau} < 2.08 \times 10^{-3}$
$h \to e\mu$ (CMS)	3.6×10^{-2}% [23]	$Y_{\mu e} < 3.85 \times 10^{-4}$

Table 1. The low energy flavour violating processes and upper limit on the Yukawa couplings. For simplicity, we assume the Yukawas $Y_{\alpha\beta} = Y_{\beta\alpha}$. The index (f) refers to the prospective future measurements.

- $h \to \mu^+\mu^-$: In Ref. [81], it is mentioned that by combining the gluon fusion and weak boson fusion channels, it is possible to obtain a 3σ significance for $h \to \mu^+\mu^-$ at an integrated luminosity of 300 fb^{-1}. It is also projected by CMS and ATLAS [82, 83] that for the 14 TeV run with an integrated luminosity of around 1200 fb^{-1}, one can observe the $h \to \mu^+\mu^-$ mode with a 5σ significance.

- $h \to \tau^+\tau^-$: Future runs of the LHC and the ILC are expected to improve the sensitivity of this coupling. From Ref. [16] one finds that the uncertainty on this coupling measurement decreases to about 12.5% and about 1.5% respectively at future runs of LHC and ILC.

- $h \to e\mu$: The improved sensitivity of MEG-II [84] will restrict $\sqrt{|Y_{\mu e}|^2 + |Y_{e\mu}|^2} \leq 4.64 \times 10^{-7}$.

- $h \to e\tau$: The future sensitivity of $\tau \to e\gamma$ with BR$\sim 10^{-9}$ will constrain the Yukawas by a further order of magnitude $\sqrt{|Y_{\tau e}|^2 + |Y_{e\tau}|^2} < 2.43 \times 10^{-3}$.

- $h \to \mu\tau$: Future experiments such as, Belle-II/super (KEK) B factory with expected sensitivity on BR$(\tau \to \mu\gamma) \sim 10^{-9}$ [85], will impose more stringent constraints on the flavour violating Yukawa $\sqrt{|Y_{\tau\mu}|^2 + |Y_{\mu\tau}|^2} < 2.41 \times 10^{-3}$.

- Finally, we briefly mention the novel proposal given in Ref. [86–88] which outlines an experimental technique to put bounds on the the flavour diagonal Higgs couplings to mostly the first generation fermions. The authors propose to achieve this by measuring isotope shifts in atomic clock transitions. This method can potentially bound the Higgs-light fermion couplings better than the present and future runs of the LHC. By studying the isotope shift of the Yb ion they show that one can bound the couplings to

$$Y_u + 1.2Y_d + 0.10Y_s \lesssim 0.04\Big(\frac{1.3 \times 10^{-3}}{Y_e}\Big)\Big(\frac{\Delta}{Hz}\Big), \tag{2.13}$$

  where Δ is the isotope shift measurement uncertainty.

We summarise the constraints from the direct searches, low energy experiments and sensitivities from the future experiments in Table 1. For simplicity, we assume that $Y_{\beta\alpha} = Y_{\alpha\beta}$ with $\alpha, \beta = e, \mu, \tau$. We find that the strongest individual constraints on $Y_{\mu\tau}$ and $Y_{e\tau}$ come from the run-I searches at the LHC. These constraints however have been obtained assuming no correlation between the two flavour violating couplings. Assuming the validity of an EFT and a non-zero $Y_{\mu\tau}$ explaining the excess seen by CMS, the limits on $Y_{e\tau}$ are strongest from a measurement of BR$(\mu \to e\gamma)$ which sets an upper limit on $|Y_{\mu\tau}Y_{e\tau}|$ at 3.98×10^{-8}. Thus, combining the excess in $h \to \mu\tau$ with the best-fit branching ratio of BR$(h \to \mu\tau) = 0.84\%$ and the MEG limit [72] on $\mu \to e\gamma$, we get $Y_{e\tau} \sim 2 \times 10^{-5}$, which is stronger than present LHC limit ($Y_{e\tau} < 1.7 \times 10^{-3}$ at 95% CL). For generic complex Yukawas, we show the constraints on Re$(Y_{e\tau})$ and Im$(Y_{e\tau})$ in Fig. 1. In the left panel, we show the existing constraints from the direct searches and the low energy experiments. The gray region is in agreement with the flavour violating low energy processes, i.e. $\tau \to e\gamma$, $\tau \to 3e$, electron EDM and electron $g-2$ as summarised in Table 1. Finally we show the combined constraint from $h \to \mu\tau$ (CMS) and $\mu \to e\gamma$ (MEG). The blue (solid) and red (dashed) lines represent BR$(h \to \mu\tau) = 1.51\%$ and 0.84% respectively. In this figure, for the charged lepton decays $\tau \to e\gamma$ and $\tau \to 3e$, we have considered the one loop contributions. The two loop contribution for $\mu \to e\gamma$ depends on the $Y_{\mu e}$ coupling and vanishes in the limit $Y_{\mu e} = 0$. In the right panel, we show the individual limits from $\tau \to e\gamma$ (pink region) and the future sensitivity from Belle-II [85] (red line) which will constrain the flavour violating Yukawa couplings by a further factor of $\mathcal{O}(0.1)$. The gray region in the right panel satisfies the constraint from $h \to \mu\tau$ and $\mu \to e\gamma$ decays, where

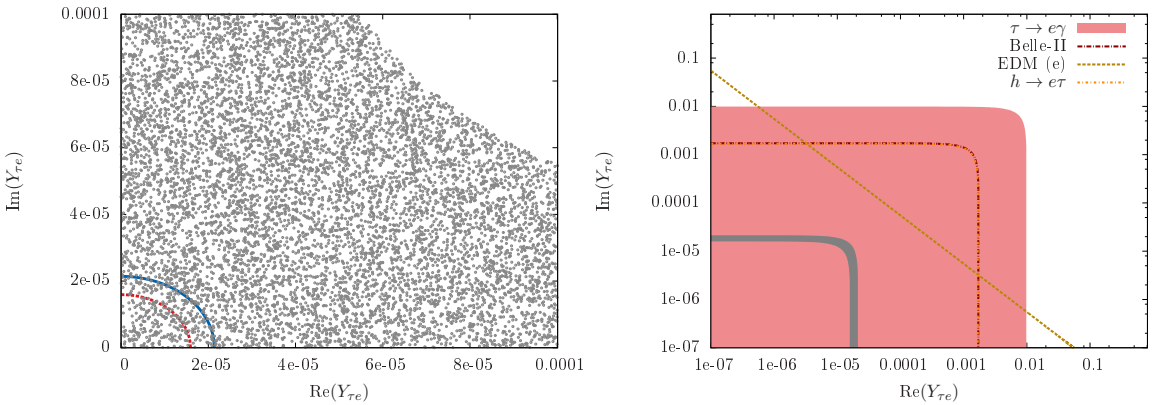

Figure 1. Figure shows the constraints on the real and imaginary parts of $Y_{\tau e}$. Left panel: The gray region (scatter plot) satisfies the flavour violating constraints $\tau \to e\gamma$, $\tau \to 3e$, electron EDM and electron $g-2$. The blue (solid) and red (dotted) lines represent the combined constraint from $h \to \tau\mu$ and $\mu \to e\gamma$ for $\mathrm{BR}(h \to \mu\tau) = 1.51\%,\ 0.84\%$ respectively. Right panel: The pink region is in agreement with the experimental limit from $\tau \to e\gamma$. The red line represents the future sensitivity from Belle-II. The gray region satisfies the combined constraints from $\tau \to e\gamma$ and $h \to \mu\tau$, where the branching ratio of $h \to \mu\tau$ varies between $0.84 - 1.51\%$.

the branching ratio of $h \to \mu\tau$ ranges from $0.84 - 1.51\%$. From Fig. 1, it is evident that the limit on $Y_{\tau e}$ is more stringent than the current LHC limit, provided that $\mathrm{BR}(h \to \mu\tau)$ lies between $0.84 - 1.51\%$ which is required to explain the excess seen by CMS. In case $Y_{\mu\tau}$ is negligibly small, then $\mathrm{BR}(h \to e\tau)$ can be as large as 0.69% from the direct LHC searches. The future sensitivity of MEG-II [84] will constrain this coupling even further. In addition, the future constraints coming from the Mu2e experiment can become even more severe [89]. However, these constraints depend strongly on the validity of the effective field theory. If the underlying degrees of freedoms are light enough, then the EFT description will not be valid [32, 40].

In the following section 3, we analyse the collider reach to probe lepton-flavour violating Higgs interactions in the $e\mu$, $\mu\tau$ and $e\tau$ decay modes for the 14 TeV LHC and its future upgrades with $3000\,\mathrm{fb}^{-1}$. Subsequently, we analyse the reach of $h \to e\tau$ at the ILC.

3 Direct detection of LFV at the HL-LHC

From the previous section, we see that the strongest constraint on $Y_{\mu\tau}$ arises from a direct search at CMS. However, the constraints from low energy measurements on $Y_{e\tau}$ and $Y_{e\mu}$ are still considerably stronger. However, it is important to note that all constraints derived from the low energy experiments are subject to correlations among various Yukawa couplings, which are innate in any EFT approach. In this section, we evaluate the high-luminosity LHC's potential to set limits on the three LFV Higgs decays, while being com-

pletely agnostic about low-energy constraints. If direct searches find evidence for both $h \to \mu\tau$ and $h \to e\tau$ in the near future - and if then as a result the bound on $|Y_{\mu\tau}Y_{e\tau}|$ is found to be weaker than obtained from the low energy experiments an interpretation in terms of an effective field theory approach will be at stake and has to be augmented with a less constraining theory assumption.

Taking a cue from Sec. 2.1, here we evaluate the possible reach of a 14 TeV high-luminosity LHC with integrated luminosities up to 3000 fb^{-1} in measuring lepton-flavour violation in the Higgs sector. Hence, we implement the relevant flavour violating interactions of the Higgs and the charged leptons in `FeynRules` [90]. The generated `Universal FeynRules Output (UFO)` [91] model is then used as input to the Monte-Carlo (MC) event generator `MadGraph5 aMC@NLO` [92]. Parton-showering and hadronisation is carried out using `Pythia 6` [93]. Thus, the τ decays are simulated using `TAUOLA` [94]. Finally we perform a detector simulations using `Delphes 3` [95] where the jets are reconstructed using the anti-k_t algorithm [96] with a jet parameter of $R = 0.5$, as implemented in `FastJet` [97]. In the following three subsections we show the prospects of each of the lepton flavour violating Higgs decays.

3.1 Prospect of $\mu\tau$ channel

In this subsection we focus on the channel where an excess of events have already been seen, *i.e.* in $h \to \mu\tau$. Among all the possible final states, e.g. $e\mu + \not{E}_T$, $\mu\mu + \not{E}_T$ and $\mu + \tau_h + \not{E}_T$, the channel where $\tau \to \mu + \not{E}_T$ is the cleanest one. In order to reduce the backgrounds, we implement the CMS-like selection cuts as listed in Ref. [22]. The different backgrounds for this final state are listed in Table. 2. The order to which these backgrounds are computed is discussed in section 3.2. For the signal, we first consider the branching ratio of $h \to \mu\tau$ as 0.84%, that corresponds to the central value for the excess reported by CMS. Hence, for the 14 TeV LHC, the signal and background events for $pp \to h \to e\mu + \not{E}_T$ with $\mathcal{L} \sim 37$ fb^{-1} are 251 and 1135 respectively. This results in a 2.1σ statistical significance. We further analyse the sensitivity reach of the HL-LHC for this channel. In Table 3, we list the number of signal and background events for an integrated luminosity of 3000 fb^{-1}. We find that this branching ratio $h \to \mu\tau$ can be constrained down to 0.76% (1.90%) with a 2σ (5σ) statistical significance. However, this can be further optimised by adding more cuts or using a multi-variate analysis. We discuss such an optimisation for the $h \to e\tau$ channel in the section 3.2.

To derive the above significances and reach, we define the statistical significance, $\mathcal{S}_1$ by assuming a flat 10% systematic uncertainty on the backgrounds

$$\mathcal{S}_1 = \frac{S}{\sqrt{S + B + \kappa^2 B^2}}, \tag{3.1}$$

where $\kappa = 10\%$ in our case. We further note that for a very low value of systematic uncertainty ($\kappa \simeq 0$), the significance is given by

$$\mathcal{S}_2 = S/\sqrt{S + B} \tag{3.2}$$

and one achieves 2σ significance for a branching ratio of $\sim 0.025\%$.

Channel	S(B) (CMS-like)	NEV_{sc}^{CMS}
$e\mu + \not{E}_T$	Signal	2421
	$\tau\tau + 1$ jet	38595
	VV	18822
	$W + 2$ jets	6517
	$t\bar{t}$	25363
	single top	1385
	SM Higgs	1319
	Total background	92001

Table 2. Signal events for BR($h \to \mu\tau$) = 0.1% after the CMS-like selection cuts. We also show the corresponding background events for the same set of cuts. The number of events are computed for $\mathcal{L} = 3000$ fb^{-1}.

Channel	BR % ($\mathcal{S}^{CMS}$)
$e\mu + \not{E}_T$	0.76 (2σ)
	1.90 (5σ)

Table 3. The lowest branching ratios BR($h \to \mu\tau$) that can be probed at 2σ and 5σ significance at the 14 TeV LHC with $\mathcal{L} = 3000$ fb^{-1}.

3.2 Prospect of $e\tau$ channel

Here we consider the flavour violating Higgs decay to $e\tau$, followed by the hadronic as well as leptonic decays of τ. For the 14 TeV $e\tau$ analysis we follow the proposal of Ref. [98] and adopt a τ tagging and mistagging efficiencies of (40%, 0.2%)[4]. Here we consider the following final states:

- $pp \to h \to e\tau \to ee + \not{E}_T$
- $pp \to h \to e\tau \to \mu e + \not{E}_T$
- $pp \to h \to e\tau \to e\tau_{had} + \not{E}_T$

The major SM backgrounds for the processes mentioned above are $\tau\tau$+ jet (computed at the next-to-next-to leading order (NNLO) [99]), VV (with $V = W^{\pm}, Z$) (at the next-to leading order (NLO) [100]), W+ jets (at NLO [101]), with W decaying leptonically and one of the jets mistagged as a τ-hadron, ee+jets (computed at NNLO [102]), $t\bar{t}$ (at next-to-next-to-next-to leading order (N^{3}LO) [103]), single-top (at NLO [104]) and the SM-Higgs backgrounds (also computed at NNLO), i.e. $h \to \tau^+\tau^-$. For the single-top background, the Wt mode has the dominant contribution for our scenario, whereas the s- and t-channel contributions are negligible. So, for simplicity, we multiplied our leading order (LO) cross-section by the NLO k-factor for the Wt mode. Besides these, there are some fake backgrounds like QCD multi-jets, where the jets might fake leptons, and $W\gamma$,

[4]Before performing the 14 TeV analysis for these three LFV decays, we validated the 8 TeV $pp \to h \to \mu\tau_{had}$ numbers as reported in the CMS run-I [22] results.

where the photon might convert to an electron-positron pair. However, it is very difficult to get a proper estimate for these backgrounds without doing a full detector simulation or without using data driven methods. For all practical purposes, these backgrounds will not significantly alter our quoted results. Hence we neglect these in the present analysis.

For the $\tau\tau+$ jet background, *viz.*, the major background for the $e\mu$ final state, we perform an ME-PS MLM matching in the MadGraph framework. For the $W+$ jets background, which is the single most important background for the $e\tau_{had}$ final state, we also simulate a matched sample with up to two partonic jets. We select only those events where at least one of the jets fake a τ-hadron. We perform an inclusive study and demand no jet veto. Similarly a matched sample was generated for the ee+jet background, which is the dominant background for the ee final state. To optimise the signal sensitivity, we adopt similar cuts as done by the CMS 8 TeV analysis for $h \to e\tau$ final state [23]. In addition, we also optimise over the p_T cuts in order to gain maximum sensitivity.

The common set of trigger cuts that we use for all the final states in this subsection are:

- The transverse momentum of e, μ and jet are: $p_T(e) > 10\,\text{GeV}$, $p_T(\mu) > 10\,\text{GeV}$ and $p_T(j) > 30$ GeV respectively,
- The pseudo-rapidity of e, μ and jet: $|\eta(e)| < 2.1$, $|\eta(e)| < 2.3$ and $|\eta(j)| < 4.7$.

We use different selection cuts for the three different final states $ee + \not{E}_T$, $\mu e + \not{E}_T$ and $e\tau_{had} + \not{E}_T$. For the $e\mu + \not{E}_T$ final state we use the following selection cuts:

- $\not{E}_T > 30$ GeV
- The azimuthal angle separations: $\Delta\phi_{\vec{\mu}-\vec{\not{E}}_T} < 0.5$ and $\Delta\phi_{\vec{\mu}-\vec{e}} > 2.7$
- The transverse mass variable: $M_T(\mu) < 65$ GeV and $M_T(e) > 50$ GeV, where the transverse mass is defined as

$$M_T(\ell) = \sqrt{2p_T(\ell)\vec{\not{E}}_T(1 - \cos\Delta\phi_{\vec{\ell}-\vec{\not{E}}_T})} \tag{3.3}$$

- The collinear mass variable: 105 GeV $< M^{\mu e}_{collinear} <$ 145 GeV, where the collinear mass is the following,

$$M_h = M_{collinear} = \frac{M_{vis}}{\sqrt{x_{\tau_{vis}}}}, \tag{3.4}$$

  with the visible momentum fraction of the τ decay products being, $x_{\tau_{vis}} = \frac{|\vec{p}_T^{\,\tau_{vis}}|}{|\vec{p}_T^{\,\tau_{vis}}|+|\vec{p}_T^{\,\nu}|}$, where $\vec{p}_T^{\,\nu} = |\vec{\not{E}}_T|\hat{p}_T^{\,\tau_{vis}}$

- In addition, we use 10 sets of cuts for p^e_T and p^μ_T optimised around the CMS-like cut, *viz.* $p^e_T > 50$ GeV and $p^\mu_T > 10$ GeV.

For the $ee + \not{E}_T$ final state, the cuts are exactly same as in the previous case with the following transformations $\mu \to e_2, e \to e_1$, where e_1 is the electron coming from the Higgs decay and e_2 comes from the τ decay. For the remaining final state $e\tau_{had} + \not{E}_T$, we use the following selection cuts:

- $\not{E}_T < 40$ GeV
- Azimuthal angle separation: $\Delta\phi_{\vec{e}-\vec{\tau}_{had}} > 2.7$ and transverse mass $M_T(\tau_{had}) < 50$ GeV
- The collinear mass: 105 GeV $< M^{e\tau_{had}}_{collinear} <$ 145 GeV
- In addition, here also we use 10 sets of cuts for p^e_T and $p^{\tau_{had}}_T$ optimised around the CMS-like cut $p^e_T > 40$ GeV and $p^{\tau_{had}}_T > 35$ GeV.

In addition to the above CMS-like selection cuts, we implement the cut on $\not{E}_T$ and the optimised p_T cut giving the maximum sensitivity (shown in Table 4). We show the number of events after all the trigger and selection cuts in Table 5 and show the exclusion limit of the BR($h \to e\tau$) in Table 6.

Channel	optimal p_T cut
$e\mu + \not{E}_T$	$p^e_T > 50$ GeV and $p^\mu_T > 10$ GeV
$ee + \not{E}_T$	$p^{e_1}_T > 50$ GeV and $p^{e_2}_T > 10$ GeV
$e\tau_{had} + \not{E}_T$	$p^e_T > 55$ GeV and $p^{\tau_{had}}_T > 50$ GeV

Table 4. Optimized p_T cuts for the three final states.

From Table 6, one can observe a BR($h \to e\tau$) of around 1.5% at 5σ for the $e\mu$ final state. For the ee final state we require a somewhat larger branching ratio to have a 5σ statistical significance. Whereas for the hadronic final state one can not go below $\sim 5.1\%$ in order to obtain a 5σ significance with such a cut-based analysis. If we statistically combine these three significances in quadrature, then we attain a 2σ significance for a branching ratio of 0.50%. Combining them additively, one achieves 2σ for as low a branching ratio as $\sim 0.32\%$. To see if one can probe lower branching ratios in the $e\mu$ channel, we exploit the kinematics of both the signal and the background in more details. We perform a multivariate analysis with the Boosted Decision Tree (BDT) algorithm using the root based TMVA [105] framework. We choose 11 kinematic variables for this purpose, *viz.*

$$|\vec{p}^{\,e}_T|,\ |\vec{p}^{\,\tau_{had}}_T|,\ \Delta\phi_{\vec{e}-\vec{\not{E}}_T},\ \Delta\phi_{\vec{\tau}_{had}-\vec{\not{E}}_T},\ \Delta\phi_{\vec{e}-\vec{\tau}_{had}},$$
$$M_T(e),\ M_T(\tau_{had}),\ M^{vis.}_{e\tau_{had}},\ M^{e\tau_{had}}_{collinear},\ \not{E}_T,\ \phi_{\vec{\not{E}}_T}.$$

For the MVA, we take care of the issue of overtraining of the signal/background. The Kolmogorov Smirnov (KS) test is used to check for the overtraining of a sample. The test sample is not overtrained if the KS probability lies between 0.1 to 0.9. In most cases, a critical KS probability value more than 0.01 [106] ensures that the signal and background samples are not overtrained.

We find after a proper training of the sample, that an optimised cut on the BDT yields a better reach on the branching ratio. In table 7, we tabulate the signal and dominant background events at an integrated luminosity of 3000 fb^{-1} after an optimised cut on the BDT variable.

Channel	S(B) (optimal)	$NEV_{sc}^{optimal}$
$e\mu + \not{E}_T$	Signal	1600
	$\tau\tau + 1$ jet	21161
	VV	7179
	$W + 2$ jets	6517
	$t\bar{t}$	12455
	single top	923
	SM Higgs	466
	Total background	48701
$ee + \not{E}_T$	Signal	1291
	$\tau\tau + 1$ jet	16636
	VV	19135
	$ee + 1$ jet	17061
	$t\bar{t}$	8605
	single top	1077
	SM Higgs	310
	Total background	62824
$e\tau_{had} + \not{E}_T$	Signal	1013
	$\tau\tau + 1$ jet	11578
	VV	2372
	$W + 2$ jets	81465
	$ee + 1$ jet	4981
	$t\bar{t}$	2038
	single top	1693
	SM Higgs	388
	Total background	104515

Table 5. Signal events for BR($h \to e\tau$) = 0.1% after all selection cuts. The superscript "*optimal*" signifies the number of events for the optimal p_T cuts. We also show the corresponding background events for the same set of cuts. The number of events are computed for $\mathcal{L} = 3000$ fb^{-1}.

Channel	BR % ($\mathcal{S}^{optimal}$)
$e\mu + \not{E}_T$	0.61 (2σ)
	1.53 (5σ)
$ee + \not{E}_T$	0.97 (2σ)
	2.44 (5σ)
$e\tau_{had} + \not{E}_T$	2.06 (2σ)
	5.17 (5σ)

Table 6. The lowest branching ratios BR($h \to e\tau$) that can be probed at 2σ and 5σ C.L.

We find that one can go down to as low as $\sim 0.48\%$ in order to achieve a 2σ significance. To achieve a 5σ discovery one can not go below a branching ratio of 1.20%. We see that

Channel	S(B) (optimal)	$NEV_{BDT}^{optimal}$
$e\mu + \not{E}_T$	Signal	277
	$\tau\tau + 1$ jet	3859
	VV	936
	$t\bar{t}$	1585
	single top	197
	Total background	6577

Table 7. Same as in Table 5 for the $h \to e\mu + \not{E}_T$ channel after an optimal cut on the BDT variable.

the MVA analysis improves the reach by a factor of ~ 1.28 for the $e\mu + \not{E}_T$ final state. We also note that in 3.2 we obtained the reach on BR($h \to \mu\tau$) with the CMS-like cuts. With an MVA, however, we expect a similar improvement in this channel as in the $e\tau$ sector.

We also note that one can attain a 2σ significance in the $e\mu + \not{E}_T$ channel with the cut-based analysis for a branching ratio of 0.028% by using Eq. 3.2.

3.3 Prospect of $e\mu$

Inspired by CMS's direct search for the flavour violating decay $h \to e\mu$ [23], we study the prospect of observing this channel at the HL-LHC. For this analysis, we apply the following simple set of cuts :

- $p_T(e) > 40$ GeV and $p_T(\mu) > 40$ GeV
- $|\eta_e| < 1.479$ and $|\eta_\mu| < 0.8$ (in the barrel)
- $\not{E}_T < 20$ GeV
- 123 GeV $< m_h <$ 127 GeV.

Here also we compute the backgrounds at the orders specified in section 3.2. The major backgrounds are $e\mu + \not{E}_T$ (dominantly from WW production), Drell-Yan production of $\tau\tau$, $t\bar{t}$, $e(\mu) + \tau + \not{E}_T$ (also dominantly from WW production), $\tau\tau + \not{E}_T$ (mainly coming from WW and ZZ) and single top (dominantly from the Wt production). In Table 8 we list the number of signal and background events after all the selection cuts for the HL-LHC at 3000 fb^{-1}. Finally in Table 9, we show the prospective reach.

Here also we note that one can attain a 2σ significance in the $e\mu$ channel with the this analysis for as low a branching ratio of 1.65×10^{-3}% by using Eq. 3.2.

4 $h \to e\tau$ at ILC

In the previous section, we discussed the prospects of observing a lepton flavour violating Higgs in all the three possible channels at a 14 TeV LHC with an integrated luminosity going up to 3000 fb^{-1}. We saw that one can definitely expect improvements compared to the 8 TeV results but due to the large backgrounds and huge uncertainties, these are

Channel	S(B)	$NEV_{sc}^{optimal}$
$e\mu$	Signal	1435
	$e\mu + \not{E}_T$	2449
	$\tau\tau$	406
	$t\bar{t}$	9511
	$e(\mu) + \tau + \not{E}_T$	152
	$\tau\tau + \not{E}_T$	5
	single top	1231
	Total background	13754

Table 8. Signal events for BR($h \to e\mu$) = 0.01% after the optimised selection cuts. We also show the corresponding background events for the same set of cuts. The number of events are computed for $\mathcal{L} = 3000$ fb^{-1}.

Channel	BR % ($\mathcal{S}$)
$e\mu$	0.0193 (2σ)
	0.0482 (5σ)

Table 9. The lowest branching ratios BR($h \to e\mu$) that can be probed at 2σ and 5σ significance at the 14 TeV LHC with $\mathcal{L} = 3000$ fb^{-1}.

not so dramatic as one would like. We know that LHC is plagued with huge backgrounds and hence we can expect better precision at lepton colliders. In this section, we repeat the analysis for $h \to e\tau$ for centre of mass energies of $\sqrt{s} = 250$ GeV and 1 TeV at an ILC machine. Here we just want to point out the improvement over the LHC. A similar improvement can be expected for the $h \to \mu\tau$ as well. For $e\mu$, we do not expect a significant improvement at ILC because in section 3.3, we already saw that the reach for the branching ratio can be as low as 1.95×10^{-2}%. The number of signal events are expected to be very low at the ILC for such small branching ratios.

The two main topologies that we study here are the associated production of the Higgs with a Z-boson and the Higgs produced in association with neutrinos through the t-channel fusion diagram. At 250 GeV, the associated production with a Z-boson offers the largest cross-section with the Z decaying hadronically, whereas for the leptonic modes of Z, the total cross-section is suppressed. Hence, we study in detail the $Zh, Z \to q\bar{q}$ production for $\sqrt{s} = 250$ GeV. For the 1 TeV study, we consider the $\not{E}h$ channel which includes both the t-channel contribution mediated by W-boson and an s-channel contribution from the Zh topology. However, here the contribution coming from the latter is nominal. The different final states that we study in this section can be summarised as :

- $e^+e^- \to Zh, h \to \tau e$, with $Z \to \geq 2j$ and $\tau \to e\nu, \mu\nu$ or τ tagged as τ_{had}
- $e^+e^- \to \not{E}h, h \to \tau e$, with $\tau \to e\nu, \mu\nu$ or τ tagged as τ_{had}.

4.1 ILC at $\sqrt{s} = 250$ GeV

In this subsection, we simulate a prospective analysis at the ILC with $\sqrt{s} = 250$ GeV. The dominant backgrounds for the various final states are:

- $Z\ell\ell\nu\nu$, $Z\ell\ell\ell\ell$ and $W\ell\nu\ell\ell$, followed by the hadronic decays of Z and W, *viz.* $Z \to q\bar{q}$ and $W \to qq'$. In short, we denote these backgrounds with the tag, $3V$-like,
- eeZ and $\tau\tau Z$, followed by $Z \to qq$. In short, we denote these backgrounds as $2V$-like, where $q =$ light jets $+ b$-jets and $\ell = e, \mu, \tau$.

Here we perform a cut-based analysis with the following set of general selection cuts:

- Demand that at least two jets reconstruct the Z-boson mass with a window of 25 GeV, i.e., $M_Z - 25$ GeV $< M_{jj} < M_Z + 25$ GeV.
- For the associated production Zh, we apply the cuts on the invariant mass of the visible products:
  - ◇ The visible invariant mass lies in 110 GeV $< M_{e\mu} <$ 140 GeV for $e\mu$.
  - ◇ The visible invariant mass lies in 120 GeV $< M_{ee} <$ 130 GeV for ee.
  - ◇ The visible invariant mass lies in 110 GeV $< M_{e\tau_{had}} <$ 140 GeV for $e\tau_{had}$.
- In addition to the above cuts, we demand a cut on $|\cos(\theta_{jj})| < 0.8$ for the $eejj$ channel in order to reduce the $2V$-like background.

In Table 10, we list the number of signal and background events after the selection cuts for the dominant modes. Finally in Table 11, we show the reach of the ILC for BR($h \to e\tau$) in these dominant final states with $\sqrt{s} = 250$ GeV. For this purpose, we use a different formula for the significance as compared to LHC, owing to the fact that the systematic uncertainties are expected to be significantly less for the ILC. We use the standard formula as quoted in the ILC Snowmass report [107], *viz.*

$$\mathcal{S} = \frac{S}{\sqrt{S+B}} \tag{4.1}$$

On statistically combining these three significances in quadrature, we attain a 2σ significance for a branching ratio of 0.38%. Combining them additively, one achieves 2σ for as low a branching ratio as $\sim 0.25\%$. So we see that the ILC at $\sqrt{s} = 250$ GeV performs comparably with the high luminosity LHC for these sets of simple cuts. To see if we have better prospects at the 1 TeV ILC, we study the vector boson fusion topology in details in section 4.2.

4.2 ILC at $\sqrt{s} = 1$ TeV

The ILC at 1 TeV motivates us to study the Higgs in association with missing energy because of much cleaner backgrounds. Another reason for studying the prospects at the 1 TeV ILC is the 1000 fb^{-1} integrated luminosity. Here, we implement the following selection cuts:

Channel	S(B) (optimal)	$NEV_{sc}^{optimal}$
$e+\mu+ \geq 2j+\not{E}$	Signal	11
	$3V-$like	14
	$2V-$like	1
	Total background	15
$2e+ \geq 2j+\not{E}$	Signal	8
	$3V-$like	4
	$2V-$like	190
	Total background	194
$e+\tau_{had}+ \geq 2j+\not{E}$	Signal	24
	$3V-$like	1
	$2V-$like	17
	Total background	18

Table 10. Signal events for BR($h \to e\tau$) = 1% and the background events after the optimised selection cuts. The above quantities are computed for $\sqrt{s} = 250$ GeV and $\mathcal{L} = 250$ fb^{-1}.

Channel	BR % ($\mathcal{S}^{optimal}$)
$e+\mu+ \geq 2j+\not{E}_T$	0.96 (2σ)
	3.39 (5σ)
$2e+ \geq 2j+\not{E}_T$	3.93 (2σ)
	> 10 (5σ)
$e+\tau_{had}+ \geq 2j+\not{E}_T$	0.44 (2σ)
	1.54 (5σ)

Table 11. Reach of BR($h \to e\tau$) at 2σ and 5σ at the ILC with $\sqrt{s} = 250$ GeV and $\mathcal{L} = 250$ fb^{-1}.

- For the $e\mu + \not{E}$ channel, we apply :
  - $1.5 < \Delta\phi_{\mu\not{E}} < 3.0$
  - The visible momentum, $|\vec{p}_{vis}| < 200$ GeV
  - $2.4 < \Delta R_{e\not{E}} < 4.0$
  - $|\cos(\theta_{e\mu}) < 0.8|$
  - The invariant mass of the visible particles, $50\,\text{GeV} < M_{e\mu} < 120\,\text{GeV}$
- For the $ee + \not{E}$ channel, we apply :
  - $2.0 < \Delta\phi_{e_1\not{E}} < 3.0$, where e_1 is the electron with the hardest p_T
  - $|\vec{p}_{vis}| < 200$ GeV
  - $2.0 < \Delta R_{e_1\not{E}} < 4.5$
  - $\Delta R_{e_1e_2} < 2.8$, where e_2 is the second hardest electron.
  - $|\cos(\theta_{e_1e_2}) < 0.8|$

◇ $100\,\text{GeV} < M_{e_1e_2} < 120\,\text{GeV}$

For the $e\tau_{had} + \not{E}$ channel, we apply :

◇ $1.5 < \Delta\phi_{\tau_{had}\not{E}} < 3.0$, where e_1 is the electron with the hardest p_T

◇ $|\vec{p}_{vis}| < 200$ GeV

◇ $2.0 < \Delta R_{\tau_{had}\not{E}} < 4.5$

◇ $60\,\text{GeV} < M_{e\tau_{had}} < 130\,\text{GeV}$,

where the notations of the variables are self-explanatory.

The dominant backgrounds for these channels can be summarised as:

- $\tau^+\tau^-$,
- $2\ell + 2\nu$ and
- 4ℓ,

where $\ell = e, \mu, \tau$.

These optimised cuts are applied to compute the significance in these three channels. We must note here that the $\Delta\phi$ distributions for the $\tau^+\tau^-$ background peak at 0 and π. Hence our $\Delta\phi$ cuts almost completely eradicate this background. The signal and background events after imposing the above sets of selection cuts are found in Table 12. The significances and the reach are summarised in table 13.

Channel	S(B) (optimal)	$NEV_{sc}^{optimal}$
$\mu + e + \not{E}$	Signal	86
	$\tau^+\tau^-$	0
	$2\ell + 2\nu$	411
	$4\ell + 2\nu$	286
	Total background	697
$2e + \not{E}$	Signal	22
	$\tau^+\tau^-$	0
	$2\ell + 2\nu$	521
	$4\ell + 2\nu$	336
	Total background	857
$e + \tau_{had} + \not{E}$	Signal	312
	$\tau^+\tau^-$	1
	$2\ell + 2\nu$	1028
	$4\ell + 2\nu$	243
	Total background	1272

Table 12. Signal events for $\text{BR}(h \to e\tau) = 1\%$ and the background events after the optimised selection cuts. The above quantities are computed for $\sqrt{s} = 1$ TeV and $\mathcal{L} = 1000$ fb^{-1}.

Channel	BR % ($\mathcal{S}^{optimal}$)
$e + \mu + \not{E}$	0.63 (2σ)
	1.68 (5σ)
$2e + \not{E}$	2.75 (2σ)
	7.22 (5σ)
$e + \tau_{had} + \not{E}$	0.24 (2σ)
	0.62 (5σ)

Table 13. Reach of BR($h \to e\tau$) at 2σ and 5σ at the ILC with $\sqrt{s} = 1$ TeV and $\mathcal{L} = 1000$ fb^{-1}.

Here also, on statistically combining the three significances in quadrature, we obtain a 2σ significance for a branching ratio of 0.22%. Combining them additively, one achieves 2σ for as low branching a ratio as $\sim 0.16\%$. We see that the ILC at 1 TeV with $\mathcal{L} = 1000\,\text{fb}^{-1}$ performs better. But, we must note that with neither scenario we can measure a branching ratio of less than 0.1%.

In doing the computations for the ILC, we consider unpolarised beams for the 250 GeV analysis because there is no significant enhancement in the signal. But for the 1 TeV analysis we consider the e^- and e^+ polarisations as (-80,20). Here we see a significant increase in the signal cross-section by ~ 2.15 times even though the dominant background, i.e. $2\ell 2\nu$ also increases by a factor of 2. So we gain in sensitivity for the polarised beams in this scenario. In contrast to the LHC studies, here we have performed a leading order analysis. However, the next-to-leading order effects are not expected to change our conclusions appreciably.

Here, we must comment on the fact that the ILC capabilities [15] on measuring an invisible branching ratio (which can very well be read as non-standard branching ratio) can be as low as 0.54% for a 250 GeV ILC machine with an integrated luminosity of 250 fb^{-1} and this decreases to around 0.22% for $\sqrt{s} = 1$ TeV with $\mathcal{L} = 1000$ fb^{-1}. As we can see that the numbers that we have obtained are in the ballpark of these quoted limits. We also mention that our analysis in the ILC sector can be further improved by optimising the cuts to a greater degree or by using a multivariate technique after identifying interesting variables.

5 Summary

The run-I results from CMS and ATLAS gave us the first hint at flavour violation in the Higgs sector in the channel $h \to \mu\tau$ with a best-fit branching ratio of less than a percent. The 8 TeV collider searches in the other two LFV channels, i.e. $h \to e\tau$ and $h \to e\mu$ did not have any significant excess over the respective SM backgrounds. Confirmation of any of these flavour violating processes will necessarily indicate the existence of new physics.

In this work, we performed rigorous collider analyses to get an estimates of the discovery prospect of all the three lepton flavour violating Higgs decays, at the high luminosity run of the 14 TeV LHC. We also performed a case study for $h \to e\tau$ at the ILC with $\sqrt{s} = 250$ GeV and 1 TeV.

Below we summarise our findings from the collider analyses.

- We analysed the prospect of $h \to \mu\tau$ and $h \to e\tau$ at the 14 TeV LHC with $\mathcal{L} = 3000$ fb^{-1} and found that a BR$(h \to \mu\tau/e\tau)$ of ~ 0.5 % can be probed with a 2σ significance.

- We obtained the prospects of observing the cleaner channel $h \to e\mu$ at the HL-LHC with an integrated luminosity of 3000 fb^{-1}. We found that to achieve a 2σ significance, one can go as low as 1.95×10^{-2}% in the branching ratio.

- In addition to the LHC, we also showed the prospects of studying Higgs flavour violation at the ILC with $\sqrt{s} = 250$ GeV and 1 TeV. A branching ratio, BR$(h \to e\tau)$ as low as 0.24% can be probed for the the $h + \not{E}$ channel with a 2σ statistical significance and with an integrated luminosity of 1000 fb^{-1} at the 1 TeV ILC. We also expect similar improvement in the $\mu\tau$ sector compared to HL-LHC.

Hence, we see that the discovery of lepton flavour violation in $h \to \mu\tau$ and/or the $h \to e\tau$ at collider experiments will imply large branching ratios of few times $\mathcal{O}(0.1\%)$. The simultaneous discovery of both these channels at the 14 TeV HL-LHC or at the ILC will no doubt question the validity of an EFT approach. This will prompt us in building models with relatively light massive states. However, if there is only evidence for one of the processes, we can not make strong statements about the existence of light degrees of freedom. Our present study thus encourages the experimental groups to look for these unique signatures and gives an estimate of the smallest branching ratios that can be probed at the near-future colliders.

Acknowledgments

We thank Cédric Delaunay, Shilpi Jain, Tanumoy Mandal and Emanuele Re for useful discussions and technical help during various phases of this work. SB acknowledges the support of the Indo French LIA THEP (Theoretical high Energy Physics) of the CNRS. The work of BB is supported by Department of Science and Technology, Government of INDIA under the Grant Agreement numbers IFA13-PH-75 (INSPIRE Faculty Award). MM would like to thank IISER Mohali, India and the DST INSPIRE Faculty award INSPIRE-15-0074. MM and MS acknowledge support by the Royal Society International Exchange 2015/R2 program.

References

[1] G. Aad *et al.* [ATLAS Collaboration], Phys. Lett. B **716**, 1 (2012) doi:10.1016/j.physletb.2012.08.020 [arXiv:1207.7214 [hep-ex]].

[2] S. Chatrchyan *et al.* [CMS Collaboration], Phys. Lett. B **716**, 30 (2012) doi:10.1016/j.physletb.2012.08.021 [arXiv:1207.7235 [hep-ex]].

[3] The ATLAS and CMS Collaborations, ATLAS-CONF-2015-044.

[4] G. Aad *et al.* [ATLAS Collaboration], Eur. Phys. J. C **76**, no. 1, 6 (2016) doi:10.1140/epjc/s10052-015-3769-y [arXiv:1507.04548 [hep-ex]].

[5] V. Khachatryan *et al.* [CMS Collaboration], Eur. Phys. J. C **75**, no. 5, 212 (2015) doi:10.1140/epjc/s10052-015-3351-7 [arXiv:1412.8662 [hep-ex]].

[6] G. Aad *et al.* [ATLAS Collaboration], JHEP **1504**, 117 (2015) doi:10.1007/JHEP04(2015)117 [arXiv:1501.04943 [hep-ex]].

[7] S. Chatrchyan *et al.* [CMS Collaboration], JHEP **1405**, 104 (2014) doi:10.1007/JHEP05(2014)104 [arXiv:1401.5041 [hep-ex]].

[8] V. Khachatryan *et al.* [CMS Collaboration], JHEP **1409**, 087 (2014) [JHEP **1410**, 106 (2014)] doi:10.1007/JHEP09(2014)087, 10.1007/JHEP10(2014)106 [arXiv:1408.1682 [hep-ex]].

[9] https://twiki.cern.ch/twiki/bin/view/CMSPublic/ttHCombinationTWiki

[10] G. Aad *et al.* [ATLAS Collaboration], Phys. Lett. B **740**, 222 (2015) doi:10.1016/j.physletb.2014.11.049 [arXiv:1409.3122 [hep-ex]].

[11] G. Aad *et al.* [ATLAS Collaboration], Phys. Lett. B **749**, 519 (2015) doi:10.1016/j.physletb.2015.07.079 [arXiv:1506.05988 [hep-ex]].

[12] G. Aad *et al.* [ATLAS Collaboration], Eur. Phys. J. C **75**, no. 7, 349 (2015) doi:10.1140/epjc/s10052-015-3543-1 [arXiv:1503.05066 [hep-ex]].

[13] G. Aad *et al.* [ATLAS Collaboration], Phys. Lett. B **738**, 68 (2014) doi:10.1016/j.physletb.2014.09.008 [arXiv:1406.7663 [hep-ex]].

[14] V. Khachatryan *et al.* [CMS Collaboration], Phys. Lett. B **744**, 184 (2015) doi:10.1016/j.physletb.2015.03.048 [arXiv:1410.6679 [hep-ex]].

[15] M. E. Peskin, arXiv:1312.4974 [hep-ph].

[16] M. E. Peskin, arXiv:1207.2516 [hep-ph].

[17] V. Khachatryan *et al.* [CMS Collaboration], Phys. Lett. B **736**, 64 (2014) doi:10.1016/j.physletb.2014.06.077 [arXiv:1405.3455 [hep-ex]].

[18] G. Aad *et al.* [ATLAS Collaboration], Eur. Phys. J. C **75**, no. 7, 335 (2015) doi:10.1140/epjc/s10052-015-3542-2 [arXiv:1503.01060 [hep-ex]].

[19] C. Englert, Y. Soreq and M. Spannowsky, JHEP **1505**, 145 (2015) doi:10.1007/JHEP05(2015)145 [arXiv:1410.5440 [hep-ph]].

[20] C. Englert and M. Spannowsky, Phys. Rev. D **90**, 053003 (2014) doi:10.1103/PhysRevD.90.053003 [arXiv:1405.0285 [hep-ph]].

[21] P. P. Giardino, K. Kannike, I. Masina, M. Raidal and A. Strumia, JHEP **1405**, 046 (2014) doi:10.1007/JHEP05(2014)046 [arXiv:1303.3570 [hep-ph]].

[22] V. Khachatryan *et al.* [CMS Collaboration], Phys. Lett. B **749**, 337 (2015) doi:10.1016/j.physletb.2015.07.053 [arXiv:1502.07400 [hep-ex]].

[23] CMS Collaboration [CMS Collaboration], CMS-PAS-HIG-14-040.

[24] https://indico.in2p3.fr/event/12279/session/5/contribution/202/material/slides/0.pdf

[25] G. Aad *et al.* [ATLAS Collaboration], JHEP **1511**, 211 (2015) doi:10.1007/JHEP11(2015)211 [arXiv:1508.03372 [hep-ex]].

[26] G. Blankenburg, J. Ellis and G. Isidori, Phys. Lett. B **712**, 386 (2012) doi:10.1016/j.physletb.2012.05.007 [arXiv:1202.5704 [hep-ph]].

[27] R. Harnik, J. Kopp and J. Zupan, JHEP **1303**, 026 (2013) doi:10.1007/JHEP03(2013)026 [arXiv:1209.1397 [hep-ph]].

[28] H. Bélusca-Maïto and A. Falkowski, arXiv:1602.02645 [hep-ph].

[29] I. Dorsner, S. Fajfer, A. Greljo, J. F. Kamenik, N. Konik and I. Niandic, JHEP **1506**, 108 (2015) doi:10.1007/JHEP06(2015)108 [arXiv:1502.07784 [hep-ph]].

[30] A. Arhrib, Y. Cheng and O. C. W. Kong, Phys. Rev. D **87**, no. 1, 015025 (2013) doi:10.1103/PhysRevD.87.015025 [arXiv:1210.8241 [hep-ph]].

[31] A. Abada, M. E. Krauss, W. Porod, F. Staub, A. Vicente and C. Weiland, JHEP **1411**, 048 (2014) doi:10.1007/JHEP11(2014)048 [arXiv:1408.0138 [hep-ph]].

[32] E. Arganda, M. J. Herrero, X. Marcano and C. Weiland, arXiv:1508.04623 [hep-ph].

[33] E. Arganda, M. J. Herrero, R. Morales and A. Szynkman, JHEP **1603**, 055 (2016) doi:10.1007/JHEP03(2016)055 [arXiv:1510.04685 [hep-ph]].

[34] C. Alvarado, R. M. Capdevilla, A. Delgado and A. Martin, arXiv:1602.08506 [hep-ph].

[35] D. Das and A. Kundu, Phys. Rev. D **92**, no. 1, 015009 (2015) doi:10.1103/PhysRevD.92.015009 [arXiv:1504.01125 [hep-ph]].

[36] M. Arroyo, J. L. Diaz-Cruz, E. Diaz and J. A. Orduz-Ducuara, arXiv:1306.2343 [hep-ph].

[37] J. Kopp and M. Nardecchia, JHEP **1410**, 156 (2014) doi:10.1007/JHEP10(2014)156 [arXiv:1406.5303 [hep-ph]].

[38] D. Aristizabal Sierra and A. Vicente, Phys. Rev. D **90**, no. 11, 115004 (2014) doi:10.1103/PhysRevD.90.115004 [arXiv:1409.7690 [hep-ph]].

[39] A. Crivellin, G. D'Ambrosio and J. Heeck, Phys. Rev. Lett. **114**, 151801 (2015) doi:10.1103/PhysRevLett.114.151801 [arXiv:1501.00993 [hep-ph]].

[40] L. de Lima, C. S. Machado, R. D. Matheus and L. A. F. do Prado, JHEP **1511**, 074 (2015) doi:10.1007/JHEP11(2015)074 [arXiv:1501.06923 [hep-ph]].

[41] S. P. Das, J. Hernndez-Snchez, A. Rosado and R. Xoxocotzi, arXiv:1503.01464 [hep-ph].

[42] Y. n. Mao and S. h. Zhu, Phys. Rev. D **93**, no. 3, 035014 (2016) doi:10.1103/PhysRevD.93.035014 [arXiv:1505.07668 [hep-ph]].

[43] F. J. Botella, G. C. Branco, M. Nebot and M. N. Rebelo, arXiv:1508.05101 [hep-ph].

[44] R. Benbrik, C. H. Chen and T. Nomura, arXiv:1511.08544 [hep-ph].

[45] Y. Omura, E. Senaha and K. Tobe, arXiv:1511.08880 [hep-ph].

[46] H. B. Zhang, T. F. Feng, S. M. Zhao, Y. L. Yan and F. Sun, arXiv:1511.08979 [hep-ph].

[47] N. Bizot, S. Davidson, M. Frigerio and J.-L. Kneur, arXiv:1512.08508 [hep-ph].

[48] M. Buschmann, J. Kopp, J. Liu and X. P. Wang, arXiv:1601.02616 [hep-ph].

[49] M. Sher and K. Thrasher, Phys. Rev. D **93**, no. 5, 055021 (2016) doi:10.1103/PhysRevD.93.055021 [arXiv:1601.03973 [hep-ph]].

[50] X. F. Han, L. Wang and J. M. Yang, arXiv:1601.04954 [hep-ph].

[51] A. Crivellin, S. Najjari and J. Rosiek, JHEP **1404**, 167 (2014) doi:10.1007/JHEP04(2014)167 [arXiv:1312.0634 [hep-ph]].

[52] A. Crivellin, M. Hoferichter and M. Procura, Phys. Rev. D **89**, 093024 (2014) doi:10.1103/PhysRevD.89.093024 [arXiv:1404.7134 [hep-ph]].

[53] A. Dery, A. Efrati, Y. Nir, Y. Soreq and V. Susi, Phys. Rev. D **90**, 115022 (2014) doi:10.1103/PhysRevD.90.115022 [arXiv:1408.1371 [hep-ph]].

[54] M. D. Campos, A. E. C. Hernndez, H. Ps and E. Schumacher, Phys. Rev. D **91**, no. 11, 116011 (2015) doi:10.1103/PhysRevD.91.116011 [arXiv:1408.1652 [hep-ph]].

[55] J. Heeck, M. Holthausen, W. Rodejohann and Y. Shimizu, Nucl. Phys. B **896**, 281 (2015) doi:10.1016/j.nuclphysb.2015.04.025 [arXiv:1412.3671 [hep-ph]].

[56] X. G. He, J. Tandean and Y. J. Zheng, JHEP **1509**, 093 (2015) doi:10.1007/JHEP09(2015)093 [arXiv:1507.02673 [hep-ph]].

[57] K. Cheung, W. Y. Keung and P. Y. Tseng, Phys. Rev. D **93**, no. 1, 015010 (2016) doi:10.1103/PhysRevD.93.015010 [arXiv:1508.01897 [hep-ph]].

[58] F. Feruglio, P. Paradisi and A. Pattori, Eur. Phys. J. C **75**, no. 12, 579 (2015) doi:10.1140/epjc/s10052-015-3807-9 [arXiv:1509.03241 [hep-ph]].

[59] D. Delepine, M. Napsuciale and E. Peinado, arXiv:1509.04057 [hep-ph].

[60] N. Konik, arXiv:1509.04590 [hep-ph].

[61] S. Baek and K. Nishiwaki, Phys. Rev. D **93**, no. 1, 015002 (2016) doi:10.1103/PhysRevD.93.015002 [arXiv:1509.07410 [hep-ph]].

[62] S. Baek and Z. F. Kang, arXiv:1510.00100 [hep-ph].

[63] L. T. Hue, H. N. Long, T. T. Thuc and N. T. Phong, arXiv:1512.03266 [hep-ph].

[64] C. F. Chang, C. H. V. Chang, C. S. Nugroho and T. C. Yuan, arXiv:1602.00680 [hep-ph].

[65] S. Davidson and P. Verdier, Phys. Rev. D **86**, 111701 (2012) doi:10.1103/PhysRevD.86.111701 [arXiv:1211.1248 [hep-ph]].

[66] D. Curtin *et al.*, Phys. Rev. D **90**, no. 7, 075004 (2014) doi:10.1103/PhysRevD.90.075004 [arXiv:1312.4992 [hep-ph]].

[67] S. Bressler, A. Dery and A. Efrati, Phys. Rev. D **90**, no. 1, 015025 (2014) doi:10.1103/PhysRevD.90.015025 [arXiv:1405.4545 [hep-ph]].

[68] C. X. Yue, C. Pang and Y. C. Guo, J. Phys. G **42**, 075003 (2015) doi:10.1088/0954-3899/42/7/075003 [arXiv:1505.02209 [hep-ph]].

[69] B. Bhattacherjee, S. Chakraborty and S. Mukherjee, arXiv:1505.02688 [hep-ph].

[70] J. Beringer *et al.* [Particle Data Group Collaboration], Phys. Rev. D **86**, 010001 (2012). doi:10.1103/PhysRevD.86.010001

[71] http://pdg.lbl.gov/2015/tables/rpp2015-sum-leptons.pdf

[72] J. Adam *et al.* [MEG Collaboration], Phys. Rev. Lett. **110**, no. 20, 201801 (2013) [arXiv:1303.0754 [hep-ex]].

[73] http://pdg.lbl.gov/2014/tables/rpp2014-sum-leptons.pdf

[74] L. Willmann *et al.*, Phys. Rev. Lett. **82**, 49 (1999) doi:10.1103/PhysRevLett.82.49 [hep-ex/9807011].

[75] T. E. Clark and S. T. Love, Mod. Phys. Lett. A **19**, 297 (2004) doi:10.1142/S0217732304013143 [hep-ph/0307264].

[76] K. Nakamura *et al.* [Particle Data Group Collaboration], J. Phys. G **37**, 075021 (2010). doi:10.1088/0954-3899/37/7A/075021

[77] G. W. Bennett *et al.* [Muon g-2 Collaboration], Phys. Rev. D **73**, 072003 (2006) doi:10.1103/PhysRevD.73.072003 [hep-ex/0602035].

[78] A. van der Schaaf, J. Phys. G **29**, 1503 (2003). doi:10.1088/0954-3899/29/8/306

[79] J. Alcaraz *et al.* [ALEPH and DELPHI and L3 and OPAL and LEP Electroweak Working Group Collaborations], hep-ex/0612034.

[80] W. Altmannshofer, J. Brod and M. Schmaltz, JHEP **1505**, 125 (2015) doi:10.1007/JHEP05(2015)125 [arXiv:1503.04830 [hep-ph]].

[81] T. Han and B. McElrath, Phys. Lett. B **528**, 81 (2002) doi:10.1016/S0370-2693(02)01208-X [hep-ph/0201023].

[82] http://www.bo.infn.it/~giacomel/talks/Higgs-Physics-prospects-LHC-LTS1-Elba-22-05-14-pg.pdf

[83] http://cds.cern.ch/record/1611186, ATL-PHYS-PUB-2013-014

[84] F. Renga [MEG Collaboration], doi:10.3204/DESY-PROC-2014-04/38 arXiv:1410.4705 [hep-ex].

[85] B. Wang [Belle-II Collaboration], arXiv:1511.09434 [physics.ins-det].

[86] C. Delaunay, R. Ozeri, G. Perez and Y. Soreq, arXiv:1601.05087 [hep-ph].

[87] C. Delaunay and Y. Soreq, arXiv:1602.04838 [hep-ph].

[88] C. Frugiuele, E. Fuchs, G. Perez and M. Schlaffer, arXiv:1602.04822 [hep-ph].

[89] R. J. Abrams *et al.* [Mu2e Collaboration], arXiv:1211.7019 [physics.ins-det].

[90] A. Alloul, N. D. Christensen, C. Degrande, C. Duhr, and B. Fuks, *FeynRules 2.0 - A complete toolbox for tree-level phenomenology*, *Comput.Phys.Commun.* **185** (2014) 2250–2300, [arXiv:1310.1921].

[91] C. Degrande, C. Duhr, B. Fuks, D. Grellscheid, O. Mattelaer, et al., *UFO - The Universal FeynRules Output*, *Comput.Phys.Commun.* **183** (2012) 1201–1214, [arXiv:1108.2040].

[92] J. Alwall, R. Frederix, S. Frixione, V. Hirschi, F. Maltoni, et al., *The automated computation of tree-level and next-to-leading order differential cross sections, and their matching to parton shower simulations*, *JHEP* **1407** (2014) 079, [arXiv:1405.0301].

[93] T. Sjostrand, S. Mrenna, and P. Z. Skands, *PYTHIA 6.4 Physics and Manual*, *JHEP* **0605** (2006) 026, [hep-ph/0603175].

[94] S. Jadach, Z. Was, R. Decker and J. H. Kuhn, Comput. Phys. Commun. **76**, 361 (1993). doi:10.1016/0010-4655(93)90061-G

[95] J. de Favereau *et al.* [DELPHES 3 Collaboration], JHEP **1402**, 057 (2014) doi:10.1007/JHEP02(2014)057 [arXiv:1307.6346 [hep-ex]].

[96] M. Cacciari, G. P. Salam and G. Soyez, JHEP **0804**, 063 (2008) doi:10.1088/1126-6708/2008/04/063 [arXiv:0802.1189 [hep-ph]].

[97] M. Cacciari, G. P. Salam and G. Soyez, Eur. Phys. J. C **72**, 1896 (2012) doi:10.1140/epjc/s10052-012-1896-2 [arXiv:1111.6097 [hep-ph]].

[98] [CMS Collaboration], CMS-PAS-TAU-11-001.

[99] R. Boughezal, X. Liu and F. Petriello, arXiv:1602.08140 [hep-ph].

[100] J. M. Campbell, R. K. Ellis and C. Williams, JHEP **1107**, 018 (2011) doi:10.1007/JHEP07(2011)018 [arXiv:1105.0020 [hep-ph]].

[101] J. M. Campbell, R. K. Ellis and D. L. Rainwater, Phys. Rev. D **68**, 094021 (2003) doi:10.1103/PhysRevD.68.094021 [hep-ph/0308195].

[102] S. Catani, L. Cieri, G. Ferrera, D. de Florian and M. Grazzini, Phys. Rev. Lett. **103**, 082001 (2009) doi:10.1103/PhysRevLett.103.082001 [arXiv:0903.2120 [hep-ph]].

[103] C. Muselli, M. Bonvini, S. Forte, S. Marzani and G. Ridolfi, JHEP **1508**, 076 (2015) doi:10.1007/JHEP08(2015)076 [arXiv:1505.02006 [hep-ph]].

[104] P. Kant, O. M. Kind, T. Kintscher, T. Lohse, T. Martini, S. Mlbitz, P. Rieck and P. Uwer, Comput. Phys. Commun. **191**, 74 (2015) doi:10.1016/j.cpc.2015.02.001 [arXiv:1406.4403 [hep-ph]].

[105] A. Hoecker, P. Speckmayer, J. Stelzer, J. Therhaag, E. von Toerne, and H. Voss, "TMVA: Toolkit for Multivariate Data Analysis," PoS A CAT 040 (2007) [physics/0703039].

[106] D. Ciupke, "Study of BDT Training Configurations with an Application to the $Z/H \to \tau\tau \to ee$ Analysis." http://www.desy.de/f/students/2012/reports/david_ciupke.pdf.gz, 2012.

[107] D. M. Asner *et al.*, arXiv:1310.0763 [hep-ph].